Investigation of nonuniformities of chemical and topological structure of space networks of synthetic rubbers using statistical analysis of tensile strength distribution curves

V. P. Dorozhkin
Kazan Institute of Chemistry and Chemical Technology, U.S.S.R., 420015, Kazan, 68, K. Marx st., USSR
(Received 29 November 1983)

A breaking strength distribution function of various synthetic rubber vulcanizates has been suggested. It has been shown that this distribution helps to determine a whole range of important characteristics of rubber destruction; namely, the most probable critical tearing surface and the number of nodes of resistance to initial microcrack propagation which are ruptured in the process of its propagation under increasing tensile load. It has been found that bimodality of the breaking strength distribution curve of some crosslinked synthetic rubbers is due to nonuniformity of the chemical and topological structure of their space networks. A qualitative fluctuation theory of the initiation of space network density nonuniformity has been put forward for castable polyurethanes.

(Keywords: rubber; network; nonuniformity; curves of strength distribution)

INTRODUCTION

Samples of any rubber always give a statistical curve of strength distribution[1,2]. Factors that may cause a spread in values are microcracks of different size in both the bulk and on the surface, various types of nonuniformity and fluctuation in the size of samples with the same shape. Kase[2] has considered the effect of the first and the third factors but totally neglected the second. However, in some cases regions with different structural strength (for example, microregions with different network types) should at least cause a bimodal strength distribution. So far as the Kase distribution is concerned, it is unimodal and cannot therefore describe a double-peak histogram of natural rubber sulphur vulcanizates[2]. This work is an attempt to describe quantitatively, strength distributions taking into account the second factor. In the statistical analysis we neglected the effect of the third factor, because dependences[3,4] which give a good description of experimental data with respect to the volume of material under study have already been obtained.

It has been established that the process of rubber tensile destruction consists of two stages. The first slow stage begins with the formation of a site of destruction due to propagation of initial microcracks of different size in the transverse direction with respect to tensile stress. As a rule, the initial tear propagation front is a circle if the site is inside the material or a semicircle if the site is on the surface. The second fast stage is observed when the critical stress defined by the limiting initial tear dimensions has been attained. Any further increase in the stress results in a rupture rate close to the velocity of sound propagation in rubber[6].

Evidently, nonuniformity of the space networks with respect to their chemical nature, functionality and density will greatly affect the slow stage of destruction. It is easy to imagine that the initial microcrack, whose propagation in time specifies the value of strength, may be found in different test samples in regions with different chemical and topological network structures. Therefore, breaking strength will depend on the type of node of resistance to initial microcrack propagation.

THEORY

Let S_{init} be the initial microcrack area, and S_{CR} the critical initial tear area (areas taken in the plane perpendicular to tension axis) through the equivalent number of nodes of resistance to the initial crack propagation covering these areas. If n is the equivalent number of nodes for initial microcracks and ν the equivalent number of nodes for critical initial tear the probability that there is a microdefect with an area of n nodes in a sample is equal to β^n (β is the probability of a microcrack whose area is equal to one node). The probability of $(\nu-n)$ nodes in the area of initial tear propagation to critical value is $\alpha^{\nu-n}$ (α is the probability of one node of resistance). Writing γ for the probability of no microdefects and us assuming that there is one unique dependence between the rupture stress σ_2 and $\nu-n$ then we have the equality

$$f(\sigma_2)\mathrm{d}(\sigma_2)=\xi(\nu-n)\mathrm{d}(\nu-n)=P \qquad (1)$$

where $f(\sigma_2)$ and $\xi(\nu-n)$ are differential distribution functions (DDF) with respect to σ_2 and $(\gamma-n)$, respectively, and P is a fraction of samples with breaking strength within $(\sigma_2+\mathrm{d}\sigma_2)$.

In accordance with the definition of the numerical distribution function (normalized to one), DDF with

0032-3861/85/060918-07$03.00

respect to $(v-n)$ is a product of the above-mentioned probabilities

$$\xi(v-n)=\gamma\cdot e^{\lambda_1 n}e^{\lambda_2(v-n)} \tag{2}$$

where $\lambda_1=\ln\beta$ and $\lambda_2=\ln\alpha$.

The integral distribution function is determined as

$$F(v-n)=\int_0^{v-n}\xi(v-n)\mathrm{d}(v-n) \tag{3}$$

and the DDF normalizing condition is expressed by

$$\int_0^{v}\xi(v-n)\mathrm{d}(v-n)=1 \tag{4}$$

Solving equations (3) and (4) leads to

$$F(v-n)=\gamma\frac{e^{\lambda_2(v-n)}e^{\lambda_1 n}-e^{\lambda_1 v}}{\lambda_2-\lambda_1} \tag{5}$$

$$1=\gamma\cdot\frac{e^{\lambda_2 v}-e^{\lambda_1 v}}{\lambda_2-\lambda_1} \tag{6}$$

The number of nodes of resistance $(v-n)$ being destroyed has the boundary values 0 and v. Consider these two extreme cases. In the case where the initial tear is on a spot with no resistance nodes and initial microdefects, the strength value must correspond to that of the initial elastomer without gel fraction and microdefects. Hence

$$\gamma e^{\lambda_1 v}=P_e \tag{7}$$

where P_e is the proportion of samples with elastomer strength within $(\sigma_e+\mathrm{d}\sigma_2)$. For the case of the presence of nodes and absence of initial microdefect, similar arguments result in the following equation

$$\gamma\cdot e^{\lambda_2 v}=P_{\sigma\mathrm{th}} \tag{8}$$

where $P_{\sigma\mathrm{th}}$ is a proportion of samples displaying the theoretical strength of the given elastomer vulcanizate. Equations (7) and (8), and expression (6) may be rewritten:

$$(P_{\sigma\mathrm{th}}-P_e)/(\lambda_2-\lambda_1)=1 \tag{9}$$

The mathematical expectation of the number of nodes ruptured during initial microcrack propagation to the critical value may be calculated from

$$(\bar{v}-n)=\gamma\int_0^{v}(v-n)e^{\lambda_1 n}\cdot e^{\lambda_2(v-n)}\cdot\mathrm{d}(v-n) \tag{10}$$

Taking into consideration equation (9) and also that $P_{\sigma\mathrm{th}}\ll P_e$ (an assumption further proved by calculating these values according to the Pearson curves), we finally obtain

$$(\bar{v}-n)=P_e^{-1}[1-e^{-P_e v}(1+P_e v)] \tag{11}$$

It follows from equations (5) and (6) that

$$v=\frac{\ln[1-(\lambda_2-\lambda_1)/P_{\sigma\mathrm{th}}]}{-(\lambda_2-\lambda_1)}\simeq\frac{\ln\left[\dfrac{P_e}{P_{\sigma\mathrm{th}}}\right]}{P_e} \tag{12}$$

$$n=\frac{\ln\left[\dfrac{(\lambda_2-\lambda_1)(F-1)}{P_{\sigma\mathrm{th}}}\right]}{-(\lambda_2-\lambda_1)}\simeq\frac{\ln\left[(1-F)\dfrac{P_e}{P_{\sigma\mathrm{th}}}\right]}{P_e} \tag{13}$$

The current value $(v-n)$ is obtainable through equations (12) and (13)

$$v-n=\frac{\ln\left[\dfrac{1}{1-F}\right]}{P_e} \tag{14}$$

Equations (11)–(14) are derived assuming that in all test samples initial tearing propagates along nodes of similar nature.

The presence of nodal microregions of another chemical or topological nature in the samples must result in initial tear propagation with a rupture of these nodes in a certain part of the vulcanizate. As a result, there appears to be a certain independent distribution curve whose shape and position are defined by the physico-mechanical characteristics of these nodes. The resultant distribution curve is a superposition of several separate distribution curves, several nodes being excited. Evidently, superposition of several distribution curves is mathematically described as follows:

$$\psi(v-n)=\sum_{L=1}^{\kappa}\varepsilon_i\cdot\xi_i(v-n) \tag{15}$$

where ε_i is the proportion of samples ruptured along i-type nodes, and ξ_i being the DDF of the i-type nodes.

The required characteristics of the generalized distribution curve may be calculated from equation (15). For example, in the case of a bimodal distribution, the methematical expectation of the total number of ruptured nodes is $(\bar{v}-n)=\varepsilon(\bar{v}-n)_1+(1-\varepsilon)(\bar{v}-n)_2$, where $(v-n)_1$ and $(\bar{v}-n)_2$ are the mathematical expectations of the number of ruptured nodes according to the first and the second curves, correspondingly.

EXPERIMENTAL

Breaking strength has been determined according to GOST 270-64. The samples tested were obtained by vulcanizing stereoregular divinyl rubber (SDR) with n-t-butyl phenol-formaldehyde resin. The vulcanizing system compositions were: divinyl rubber 100 parts by wt., stearic acid 1.0 part by wt., chlorosulphonated polyethylene 4.0 parts by wt., ZnO 3.0 parts by wt., technical carbon DG-100 50.0 parts by wt., resin 101 8.0 parts by wt.

Rubber mixtures were prepared on mills, with water cooling to 13°C and mill friction—1.2. Conditions of the preparation of the five samples used are listed in *Table 1*.

The rubber mixtures were vulcanized in an electroheated press at 160°C for 30 min. No less than 150 samples were tested on a tensile testing machine.

Stereoregular isoprene rubber (SIR) was vulcanized at 133°C for 20 min. The mixture composition was (in parts by weight): isoprene rubber 100.0, sulphur 1.0, altax 0.6, diphenylguanidine 3.0, stearic acid 1.0, ZnO 5.0, neozone D 0.6.

Urethane rubbers crosslinked by different methods were also used and tensile-tested for strength. CKY-8 urethane millable rubber was obtained from polyethylene–propyleneadipateglycol (PEPG) polyester, 2,4-toluenediisocyanate (2.4-TDI) and 1.4-butanediol as

elongating agent. The molar ratio of OH-groups to NCO-groups was close to one. CKY-8 PG was vulcanized with the organic peroxide of α,α'-di-t-butylperoxi-1,4-diisopropylbenzene (peroximon F-40) at 153°C for 30 min. The rubber mixture composition was as follows (parts by weight): urethane rubber CKY-8 (PG 100.0; stearic acid 1.0; peroximon-F-40 10.0; technical carbon TM-75 40.0.

CKY-PF castable urethane rubber was obtained using polyoxitetramethyleneglycol polyether (POTMG) in the following manner: a prepolymer with an end NCO-group was synthesized by reacting 1.0 mole of POTMG and 2.0 moles of 2.4-TDI; the pre-melted aromatic diamine 4,4'-methylenecortobischloraniline (MOCA) was added to the prepolymer in a proportion of 0.8 mole per 1.0 mole of the prepolymer. The reaction mixture was stirred for 10 min at 65°C and then cast into moulds. The filled moulds were kept in a constant temperature cabinet at 80°C for 48 h. After two weeks storage at room temperature the 150 samples were tensile-tested.

CKY-PE, a castable urethane rubber based on polyethylenedipateglycol (PEA) polyester, was obtained by two different methods: (1) a single stage process in which all of the components were charged into a reactor simultaneously; (2) a double-stage process in which the 2,4-TDI was added to desiccated PEA polyester and the synthesis carried out at 80°C for 30–40 min. The molar ratio of the components used was 1.0 PEA to 2.0 TDI to which 0.8 moles of melted MOCA were added over a period of 10 min at 65°C. In both cases the composition obtained was case into moulds and kept at 80°C for 48 h in constant temperature cabinets. Prior to physico–mechanical tests the samples were stored for 14 days at room temperature.

To determine Young's modulus of the synthetic rubber vulcanizates, samples in the shape of 0.1–0.15 mm thick and 3.0 mm wide films were cooled to a temperature 30°C–40°C below the vitrification temperature and subjected to uniaxial tension within 0.05–0.2%. The degree of deformation was determined with the help of an optical system which makes it possible to detect a degree of deformation as small as 10^{-6} m. Low temperature and small degree of deformation allow the assumption to be made that the entropy component contribution to deformation is negligible, and that the measured moduli reflect only elastic deformation. In order to determine the value of the tensile stress rubbers without gel-fractions and microdefects, a piece of rubber was dissolved and the solution repeatedly filtered. Rubber films not more than 0.1 mm thick were then obtaned by evaporating the solvent under vacuum conditions. Tensile strength of a film strip 1.0 mm wide was determined with respect to the extension of a calibrated spring. The density of cross bonds in vulcanizates v_e/v was determined by equilibrium compression according to Cluff–Gladding[7].

DISCUSSION

Figure 1 presents the breaking strength distribution curves of divinyl rubber vulcanizates, plotted on the basis of experimental histograms. As can be seen from *Figure 1*, curves 2–4 have a clearly marked bimodal distribution, a result of superposition of two distribution curves. The share of the first curve increases with milling time. This fact makes it possible to assume that mechanical mixing for more than 17 min results in the formation of space network regions of a new nature in bulk SDR vulcanizate. If the milling time is sufficiently long, the latter type of nodes increases so that some unique structure with chaotic location of the nodes of new nature is formed. This determines the regeneration of a unimodal distribution curve (curve 5).

In order to calculate the mean statistical number of ruptured nodes and, consequently, the critical initial tear area we have to know $P_{\sigma th}$ and P_e for every type of synthetic rubber. A method of describing unimodal distribution curves by Pearson curves has been used to determine these values[8]. Bimodal curves were graphically divided into unimodal curves. It appeared that the experimental curves and those obtained by graphic division of the unimodal distribution curves are described by the Pearson curve functions of the 7th type. To calculate the values of $P_{\sigma th}$ and P_e according to the Pearson curve functions, in addition to the tensile strength of rubber without gel fraction and microcracks, we must know the theoretical strength of the vulcanizates. Orowan[9] and Kobeko[10] have shown that the theoretical strength σ_{th} can be approximately calculated from

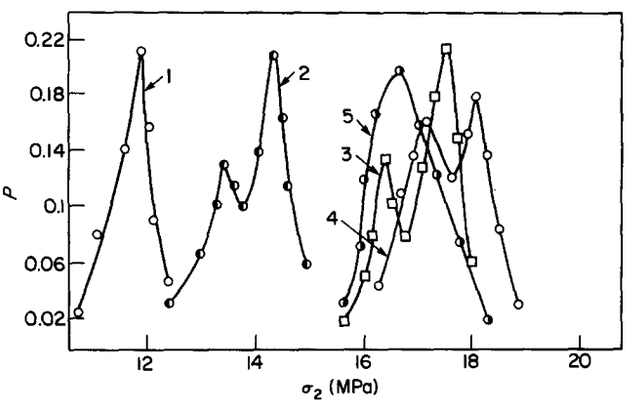

Figure 1 Experimental breaking strength distribution curves of SDR vulcanizates (curves are itemized under numbers of mixtures from which corresponding vulcanizates are obtained)

Table 1 Mixture preparation conditions

Mixture No.	Introduction time (minutes)					Total preparation time of rubber mixture (minutes)
	Stearic acid	Chlorosulphonated polyethylene	ZnO	DG-100	Resin 101	
1	2	2	2	7	2	17
2	2	2	2	10	3	21
3	2	3	3	15	5	30
4	2	4	4	20	7	39
5	2	5	5	21	8	43

$$\sigma_{th} \approx 0.1 \cdot E \quad (16)$$

where E is Young's modulus. Inasmuch as the degree of $P_{\sigma th}$ has influence on n and v in formulae (12) and (13) is insignificant compared with that of P_e, then such an approximation is satisfactory. The number of nodes n and v can be expressed in terms of the area they occupy, if we know the density of the vulcanizate space network and assume that the nodes are evenly distributed in the vulcanizate.

Table 2 presents some calculated data on SDR resin vulcanizates.

A survey of *Table 2* shows that an increase in milling time to 39 min results in an increase in the number of nodes of a new kind. The critical initial tear area S_{CR} also increases. It seems that the new nodes are physico-chemical black rubber bonds, because according to *Table 2* the area per one such node is 50–100 Å^2, which agrees well with the data presented in ref. 11. Milling of rubber mixtures for more than 30 min reduces the efficient density of cross bonds. This phenomenon necessitates an ever increasing mechanical destruction of SDR rubber macromolecules. It is interesting to note that the density of black rubber bonds (peaks 1) is by an order of magnitude greater than that of vulcanization bonds (peaks 2).

A definite dependence can be observed between the number of nodes of resistance to initial tear propagation and SDR vulcanizate strength. The rupture stress σ_2 grows with $(\bar{v}-n)$. Assuming that the dependence between $(v-n)$ and σ_2 is expressed by

$$\sigma_2 = K(\bar{v}-n)^b + \sigma_c \quad (17)$$

where K and b are constants characteristic of each vulcanizate type.

With respect to σ_2, DDF has the form of $f(\sigma_2) = \frac{\xi(v-n)\mathrm{d}(v-n)}{\mathrm{d}\sigma_2}$ or using (7) and (9)

$$f(\sigma_2) = P_c \exp[(P_{\sigma_{th}} - P_c)(v-n)] \frac{\mathrm{d}(v-n)}{\mathrm{d}\sigma_2} \quad (18)$$

From equation (17), and bearing in mind that $P_{\sigma_{th}} \ll P_c$ (for mixture 1 vulcanizates these values are the closest and are $2.8 \cdot 10^{-12}$ and $2.2 \cdot 10^{-8}$, correspondingly) we get the final form of DDF with respect to σ_2

$$f(\sigma_2) = 1bK^{-1/b}(\sigma_2 - \sigma_c)^{(1/b-1)} P_c \exp\{-P_c[(\sigma_2 - \sigma_c)/K]^{1/b}\} \quad (19)$$

To calculate $f(\sigma_2)$ we only have to know the values of P_c, b and K. In the case of a multimodal distribution, the values of the K and b constants are found for each individual curve constituting the integral DDF.

With the help of equation (19) we can calculate theoretical values of a relative number of samples which have displayed strength within $\sigma_2 + \mathrm{d}\sigma_2$ according to $P = f(\sigma_2)\mathrm{d}\sigma_2$. Multiplying P by the total number of tested samples, we can obtain the theoretical occurrence of samples which have displayed breaking strength within any interval. *Table 3* shows the experimental and theoretical values of the occurrence of frequencies of various σ_2 of vulcanizates from mixtures 1 and 2.

Theoretical and experimental data agree well. This proves that the assumption that the σ_2 on $(\bar{v}-n)$ dependence is expressed through equation (17) which may be considered correct to a first approximation.

We have checked the Kase equation for applicability to our vulcanizates

$$\sigma_2 = \sigma_{th}(1 - \theta \cdot x) \quad (20)$$

where x is the initial microcrack area and θ is a positive

Table 2 Some experimental and calculated data on SDR resin vulcanizates

Mixture no.	Contribution of each distribution to total probability density	$S_{CR}^* \cdot 10^6$ cm^2	$(v-n) \cdot 10^{-9}$	$(v-n)_{av}^* 10^{-9}$	$\gamma_c/v \cdot 10^{20}$ (cm^3)$^{-1}$	σ_2^* MPa
1	1.0	8.81	0.058	0.058	3.15	11.9
2 peak 1	0.21	34.18	0.66	0.256	3.4	14.2
peak 2	0.79		0.14			
3 peak 1	0.228		5.48			
peak 2	0.77	135.37	0.28	1.47	3.93	17.3
4 peak 1	0.31		3.65			
peak 2	0.69	166.02	0.336	1.36	3.19	18.2
5	1.0	72.6	0.429	0.429	2.92	16.9

* Calculated through equation (15)

Table 3 Distribution of ruptured stress values of SDR vulcanizates

Mixture 1 vulcanizates			Mixture 2 vulcanizates		
Stress intervals (MPa)	Observed occurrence	Theoretical occurrence	Stress intervals (MPa)	Observed occurrence	Theoretical occurrence
–10.4	4.0	2.0	–12.4	4.0	1.0
10.4–10.7	11.0	7.5	12.4–12.7	6.0	5.7
10.7–11.0	20.0	15.0	12.7–13.0	11.0	10.9
11.0–11.3	23.0	23.0	13.0–13.4	22.0	22.8
11.3–11.6	28.0	27.9	13.4–13.7	16.0	19.3
11.6–11.9	34.0	33.7	13.7–14.1	22.0	23.5
11.9–12.2	22.0	23.4	14.1–14.4	36.0	26.2
12.2–12.5	8.0	17.0	14.4–14.8	23.0	26.2
			14.8–15.1	10.0	18.4
Total	150	150	Total	150	150

constant. Equation (20) may be rewritten

$$\sigma_2 = \sigma_{th}\left[1-\left(1-\frac{\sigma_c}{\sigma_{th}}\right)\frac{n}{\nu}\right] \quad (21)$$

where $\theta = 1-\sigma_c/\sigma_{th}$, because at $n=0$ (ν) the rupture stress σ_2 must be equal to $\sigma_{th}(\sigma_c)$. Taking into account equations (1), (2) and (21) we may obtain DDF with respect to σ_2. Calculations performed on the basis of this function have however shown poor agreement of experimental and theoretical occurrences.

Experiments and calculations similar to those presented above for SDR vulcanizates have been performed for SIR isoprene rubber sulphur vulcanizates. Analysis of the curves on the basis of equations (12)–(14), using $\sigma_c = 0.44$ MPa, $\sigma_{th} = 166$ MPa, and $\nu_c/\nu = 1.327\cdot10^{20}\,(cm^3)^{-1}$, has given the following results: $S_{CR} = 0.96\cdot10^{-6}$ cm^2 and the most probable number of ruptured nodes in the area of initial tear propagation is $0.816\cdot10^7$. Comparison of these data with *Table 2* shows that the number of nodes ruptured in SIR vulcanizates is hundreds of times smaller than that in SDR. This is ascribed to the fact that SIR unfilled vulcanizates do not have black rubber bonds. Considering that SIR vulcanizates are somewhat stronger than SDR vulcanizates, it may be assumed that SIR vulcanization nodes of resistance offer more resistance to microcrack propagation. This becomes clear when we take into account that physico-mechanical adhesion between technical carbon and rubber is much weaker than between actual network vulcanization nodes[13]. A dependence between σ_2 and $(\nu-n)$ for SIR vulcanizates is described by equation (17), constant values being $K = 125.17$ and $b = 0.0649$. *Table 4* presents experimental and theoretical values for SIR sulphur vulcanizate rupture stress occurrences.

Despite the good agreement between the experimental and theoretical results, these values differ greatly in the initial and end regions of breaking strength distribution. For example, within the σ_2 range of SIR from 27.16 MPa to 34.84 MPa the dispersion (S^2) of theoretical occurrence (n^{th}) from experimental (n^{exp}) is 0.18, whereas S^2 for σ_2 for the beginning and end of the distribution is 2.33, i.e. nearly 13 times greater. S^2 was calculated from

$$S^2 = \frac{\sum_{i=1}^{n}\left(\frac{n_i^{exp}-n_i^{th}}{n_i^{exp}}\right)^2}{n}$$

where n is the number of stress intervals.

Similar calculation of S^2 for SIR vulcanizates (*Table 3*, mixture 1) gives 0.016 for σ_2 within 10.7 MPa – 1.2 MPa; for other σ_2 values the dispersion is 20 times greater ($S^2 = 0.317$). Close results have been obtained for SDR vulcanizates from mixtures 2–5 (*Table 1*).

The data on S^2 variances show that equation (17) correctly reflects the dependence of $\bar{\sigma}_2$ on $(\nu-n)$ only in the interval $\bar{\sigma}_2 \pm \sigma$ where σ_2 is the mean arithmetic value of breaking strength of the given vulcanizate, σ is the root square of breaking strength variance:

$$\sigma^2 = \frac{\sum_{i=1}^{n}(\bar{\sigma}_2-\sigma_{2i})^2}{n-1}$$

where σ_{2i} is a mean value of stress of the i-th interval.

Beyond these limits the rupture stress value is specified not only by quality, nature and topology of nodes of resistance to microcrack propagation, but also, probably, by a range of other physico-chemical characteristics of the material. In the region of small values of σ_2 it is, in the first place, cohesion of rubber from which a vulcanizate is prepared. Besides, the value of friction between interlaced rubber macromolecules significantly influences the value of σ_2 in this region. For samples with σ_2 higher than $\bar{\sigma}_2+\sigma$ the degree of chemical and physical structure organization should also be taken into consideration. All these problems, though, are beyond the scope of this report and will be dealt with in greater detail later.

Of special interest are the experimental results obtained on crosslinked polyurethanes. *Figure 2* presents DDF with respect to σ_2 of four crosslinked polyurethane rubbers. A significant difference in the distributions of CKY-8PG rubber peroxide vulcanizate and CKY-PE and CKY-PF castable rubbers should immediately draw attention. This difference is due to urethane rubber macromolecule propagation and crosslinking step sequences. In the case of CKY-8PG the millable linear polyurethane or poorly branched macromolecules are obtained initially. Then, when a rubber mixture is prepared, they are crosslinked by organic peroxide. In the case of castable polyurethane preparation, macro-

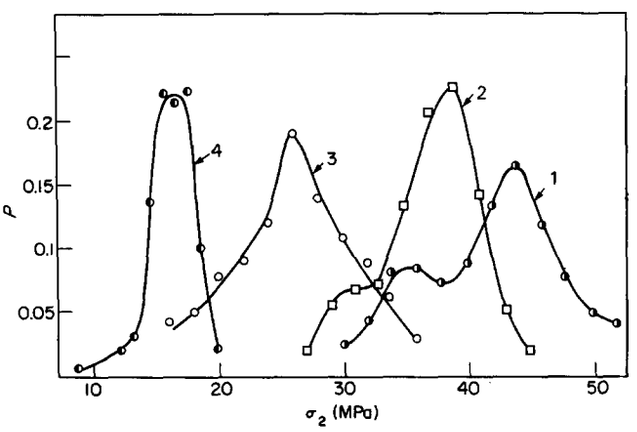

Figure 2 Experimental breaking strength distribution curves of urethane rubber vulcanizates. (1) CKY-PE, single-stage process; (2) CKY-PE, double-stage process; (3) CKY-PF; (4) CKY-8PG

Table 4 Distribution of rupture stress values occurrences of SRI vulcanizates

Stress invervals (MPa)	Observed occurrence	Theoretical occurrence	Stress intervals (MPa)	Observed occurrence	Theoretical occurrence
–25.8	6	4.2	31.00–32.28	31	26.0
25.8 –27.16	8	9.0	32.28–33.56	15	27.8
27.16–28.44	20	18.8	33.56–34.84	10	7.3
28.44–29.72	23	26.6	34.84–36.12	3.0	5.4
29.72–31.00	33	31.4	36.12–37.40	1.0	3.5

molecule propagation, branching and crosslinking steps proceed practically simultaneously[14] and the results in a greater nonuniformity of the network structure. Nonuniformity of the network and a less regular chemical structure of macrochains results, not only in broadening of the DDF curve, but also in a significant change in other properties of polyurethanes. For example, a single stage method of preparing[15] crystalline polyurethanes gives a wider melting interval compared with a double-stage preparation. A whole range of physico–mechanical properties are more evident in the case of a single-stage method[16,17]. It is also evident from *Figure 2*, that the value $\bar{\sigma}_2$ calculated through equation (15) is greater for a single-stage process (curve 2, $\sigma_2 = 42.0$ MPa) than a for a double-stage process (curve 1, $\bar{\sigma}_2 = 37.85$ MPa). Several interesting facts concerning polyurethane preparation step sequence effects are presented in a recently published work by Dušek[18]. It appeared that in the case of a double-stage method, microphase division is less clearly defined, whereas cyclization is much more evident than in the case of a single-stage method. All these facts indicate the great difference in the chemical and topological structure of polyurethanes obtained by different methods. The reason for this difference is not simply the step sequence, but complex dynamics of various chemical and physical processes occurring in the course of crosslinked polyurethane production. In summary the complex process of castable polyurethane formation may be presented in the following way. As linear macromolecule propagation proceeds and the molecular weight reaches a certain value, branching[14] and then crosslinking begin. At this moment the microgel formation stage begins. It should be noted that microgel formation may begin even at low degrees of conversion, a fact verified by a microbreakdown of the reaction system with the formation of colloidal particles[19], whose number and size change with time. It would be logical to consider that up to the microgel formation stage the rate of urethane formation is defined by chemical kinetics, and after, by diffusion kinetics. On reaching some critical size microgel particles are united by crosslinking and form a single macrogel. Such networks formed according a heterogeneous mechanism are less regular in comparison with those formed in the case of homogeneous formation of spatial structure. It may be assumed that branching and crosslinking of linear macromolecules into a colloid-size microgel is a homogeneous process.

The above scheme of formation of the castable polyurethane network structure is at odds with the established experimental fact, namely, the region of chemical kinetics of urethane formation extends at least to 95% conversion[20], that is, practically to the end of the process, because it is known that bulk polycondensation rarely exceeds 97% conversion. Consequently, the assumption that the entire structuralization process is homogeneous is more legitimate. In this case the pattern of crosslinked polyurethane formation may be presented as follows: there are microregions with increased NCO-group content in the reaction mixture due to density fluctuation and the NCO-group concentration fluctuation time is comparable with or even exceeds the elementary interaction time of this group with other reaction groups present in the reaction mixture. If this is true, then microregions with increased or reduced NCO-group content may appear in the reaction mass. Naturally, the relation between propagation, branching and crosslinking of macromolecules in these regions will differ from the relation between these reactions in the entire system. As urethane formation proceeds and viscosity increases, the density fluctuations may be fixed in separate microregions for ever longer periods. The chemical and topological structures obtained in these regions will be different. In microregions with higher NCO-group contents, there may appear in the early stages crosslinked structures, whereas in regions with lower NCO-group content short linear micromolecules are most probable.

The degree of conversion of groups capable of reacting with NCO-groups in regions with well-branched or even crosslinked macromolecules is close to 100% even at low conversion. Therefore, further urethane formation continues as a homogeneous reaction but on this occasion mainly in regions with linear and poorly-branched macromolecules. NCO-group concentration fluctuation cannot be excluded in these regions, though not in the form of initial diisocyanate, but mainly as macromolecule end groups. The above pattern of initiation of various chemical and topological structures is repeated but on a quantatively different level. Thus, microgel particles may be detected at various stages of urethane formation, but their size will differ depending on conversion. The size of particles will grow with conversion and when the degree of conversion reaches its critical value, the particles become so big that they merge into a single macrogel due to reactions of the NCO-groups present in the surface layers of microgel particles. A small fraction of microgel particles is probably united by long macromolecules whose various sections are integrated into different particles. After a macrogel is formed, further urethane formation proceeds in a sol fraction according to the laws of chemical kinetics. Reactions may also proceed in the gel fraction, but their proportion is insignificant owing to spatial limitations imposed by the crosslinked structure. It is for these reasons that the chemical kinetics region extends to 95% conversion, and that a 100% conversion is rarely attainable.

Let us consider the shapes of DDF curves with respect to σ_2 of various castable polyurethanes from the point of view of the above statements. CKY–PE samples are characterized by a bimodal distribution curve, bimodality being markedly stronger in a single-stage polyurethane production process. This may be ascribed to the fact that in the case of a simultaneous charging of low-molecular diisocyanate and aromatic diamine the probability of NCO-group concentration fluctuation is much higher than when using a system with a pre-polymer with end NCO-groups (a double-stage method). It is clear that prepolymer density fluctuation will occur much less frequently than low molecular diisocyanate fluctuation. In this case nonuniformity of chemical and topological structures will be more marked than in the case of a single-stage process. It is especially characteristic of such important properties of crosslinked polymers such as crosslink density which is indirectly connected with σ_2 in equation (17). In fact, if the initial microcrack propagates to the critical value in a region with a denser space network, then its propagation will be resisted by a greater number of nodes of resistance $(\nu - n)$ than in a region with a less dense network. It is due to a greater nonuniformity of the space network that the C fraction of the first distribution curve with respect to σ_2 ($C = 0.21$) of a single-

stage process is considerably greater than that of a double-stage process ($C = 0.1$). The unimodality of DDF with respect to σ_2 for a CKY–PF rubber seems to be connected with the better unformity of the topological network structure of the ether based castable polyurethane.

CONCLUSION

Briefly summing up the presented experimental and theoretical material, it is possible to conclude that there is a great nonuniformity of chemical and topological network structures in a range of crosslinked synthetic rubbers. This nonuniformity is detected by simple tensile strength test experiments.

REFERENCES

1 Bartenev, G. M. and Brukhanov, L. S. *Teknich. Phis.* 1958, **28**, 288
2 Kase, S. *J. Polym. Sci.* 1953, **II**, 425
3 Cumbrell, E. J. 'Statistics of Extremes', Publishers?, New York, 1958
4 Weibull, W. 'Fatigue Testing and the Analysis of Results', Publishers?, New York, 1961
5 Bartenev, G. M. and Belostotskaia, G. I. *Z. Teknich. Phis.* 1954, **24**, 1773
6 Gul', V. E., Krutetskaya, G. P. and Kovriga, V. V. *Kauch. Resin.* 1957, **N12**, 1
7 Cluff, E. and Cladding, E. *J. Polym. Sci.* 1960, **18**, 341
8 Mitropolsky, A. K. 'Tekhnika Statisticheskih Vychesleniy', Moskva, Izdatelstvo 'Nauka', 1971
9 Orowan, E. *Nature* 1944, **154**, 341
10 Kobeko, P. P. 'Amorphnyie Veshestva', Moskva, Izdatelstvo AN SSSR, 1952
11 Dorozhkin, V. P., Kimelblat, V. I. and Averko-Antonovich, Y. O. *Vysokomol. Soedin.* 1974, **A16**, 2024
12 Spravochnik Rezinshika, Moskva, Izdatelstvo, 'Khimiya', 1971
13 Parkinson, D. *J. Appl. Phys.* 1951, **2**, 273
14 Dorozhkin, V. P. and Alexandrova, T. V. *Vysokomol. Soedin.* 1977, **A19**, 853
15 Panova, N. V., Muller, B. E., Apukhtina, N. P. *Vysokomol. Soedin.* 1971, **B13**, 129
16 Lipatova, T. E., Ivashenko, V. K. and Bezruk, L. I. *Vysokomol. Soedin.* 1971, **A13**, 1701
17 Rausch, K. W. and Sayigh, A. A. *Ind. Eng. Chem. Prod. Res. Dev.* 1965, **4**, 92
18 Matëjka, L. and Dušek, K. *Polym. Bull. B.* 1980, **N819**, 489
19 Nesterov, A. E., Lipatova, T. E., Zubko, S. A. and Lipatov, Y. S. *Vysokomol. Soedin.* 1970, **A12**, 2253
20 Olkhov, Y. A., Baturin, S. M. and Entelis, S. G. *Vysokomol. Soedin.* 1976, **A18**, 150